Current Biology *16*, 1944–1949, October 10, 2006 ©2006 Elsevier Ltd All rights reserved DOI 10.1016/j.cub.2006.08.029

Report

Katanin Disrupts the Microtubule Lattice and Increases Polymer Number in *C. elegans* Meiosis

Martin Srayko,[1,3] Eileen T. O'Toole,[2,3] Anthony A. Hyman,[1] and Thomas Müller-Reichert[1,*]
[1] Max Planck Institute of Molecular Cell Biology and Genetics
D-01307 Dresden
Germany
[2] Boulder Laboratory for 3-D Electron Microscopy of Cells
University of Colorado
Boulder, Colorado 80309

Summary

Katanin is a heterodimer that exhibits ATP-dependent microtubule-severing activity in vitro [1, 2]. In *Xenopus* egg extracts, katanin activity correlates with the addition of cyclin B/cdc2, suggesting a role for microtubule severing in the disassembly of long interphase microtubules as the cell prepares for mitosis [3, 4]. However, studies from plant cells [5, 6], cultured neurons [7], and nematode embryos [8, 9] suggest that katanin could be required for the organization or postnucleation processing of microtubules, rather than the dissolution of microtubule structures. Here we reexamine katanin's role by studying acentrosomal female meiotic spindles in *C. elegans* embryos. In mutant embryos lacking katanin, microtubules form around meiotic chromatin but do not organize into bipolar spindles [8, 9]. By using electron tomography, we found that katanin converts long microtubule polymers into shorter microtubule fragments near meiotic chromatin. We further show that turning on katanin during mitosis also creates a large pool of short microtubules near the centrosome. Furthermore, the identification of katanin-dependent microtubule lattice defects supports a mechanism involving an initial perforation of the protofilament wall. Taken together, our data suggest that katanin is used during meiotic spindle assembly to increase polymer number from a relatively inefficient chromatin-based microtubule nucleation pathway.

Results and Discussion

To examine the effect of katanin on microtubule morphology in *C. elegans* meiosis, we performed electron tomography and 3-D modeling of female meiotic spindles in wild-type and a *mei-1(null)* mutant that lacks katanin activity (Figure 1). We tracked microtubules and identified their ends within a half spindle, built from two serial 400 nm thick sections. Surprisingly, the pole-facing microtubule ends in wild-type meiosis were not found exclusively at the spindle pole, but were distributed throughout the volume of the spindle (Figure 1C, white spheres; see Movie S1 in the Supplemental Data available online). Similarly, chromatin-facing microtubule ends were not concentrated at the chromosome surfaces, but were also observed throughout the spindle (Figure 1C, blue spheres; Movie S1). The wild-type meiotic spindle contained many short microtubules, most of which were aligned and oriented along the spindle axis.

Next, we looked at microtubules surrounding meiotic chromatin in a *mei-1(null)* mutant. Under conditions in which organized spindles were not formed (Figure 1B), relatively few microtubules were found around the chromatin compared to the wild-type spindle (73 versus 348, respectively Figures 1C and 1D; also see Movies S1 and S2). Most of the microtubules in the *mei-1(null)* data set extended beyond the volume, and the total amount of microtubule polymer in *mei-1(null)* was reduced compared to wild-type (Figure 1E). Consistent with this observation, antitubulin-immunostained embryos displayed a significant reduction in tubulin immunofluorescence intensity within a defined area around meiotic chromatin in *mei-1(null)* mutant embryos, as compared to wild-type ($p = 5E\text{-}06$, Figure S1). Length measurements of microtubules completely contained within the volume of the tomographic reconstruction indicated a sharp decrease in the number of microtubules <200 nm long, indicating that katanin activity itself, or post-severing events, are regulated so that microtubule fragments in the 200–500 nm range accumulate (Figure 1F). Therefore, in contrast to the idea that katanin is required to disassemble microtubule arrays (for instance during the interphase to mitosis transition [3]), our results suggest that katanin contributes to an increase in the steady-state number of microtubules and an increase in total polymer amount in wild-type meiotic spindles.

One explanation for the above result is that katanin-mediated severing converts long microtubules into two or more smaller polymers that are relatively resistant to depolymerization. We searched for evidence of microtubule severing by examining individual microtubules in wild-type meiotic spindles and compared those to microtubules in the *mei-1(null)* mutant. By stepping through serial 1.6 nm tomographic slices, two morphological differences in microtubules were unique to wild-type: lateral defects ("holes") within the microtubule lattice of varying sizes and closely opposed open microtubule ends. Microtubules with lateral defects in their protofilament lattice were found throughout the wild-type spindle (Figure 2A and Movie S3). In addition, numerous microtubules showed more than one lateral defect along their length. Significantly, we did not observe any of these structures in the *mei-1(null)* mutant. We used these observations to estimate katanin's contribution to the fragmentation of spindle microtubules by dividing the total polymer length within the reconstructed volume by the number of lateral defects and closely opposed ends. In the wild-type reconstruction,

*Correspondence: mueller-reichert@mpi-cbg.de
[3] These authors contributed equally to this work.

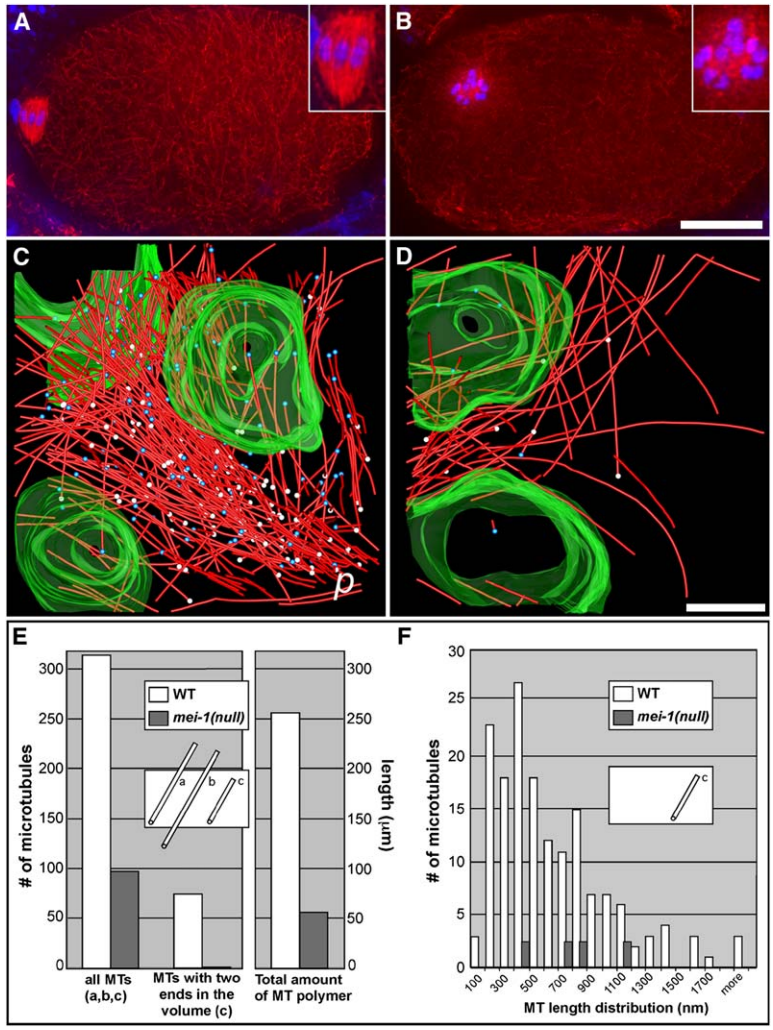

Figure 1. MEI-1 Generates Numerous Microtubules in Meiotic Spindles

(A and B) Images of wild-type (A) and *mei-1(null)* (B) embryos fixed and immunostained with anti-α-tubulin (red) are shown. DNA (blue) is visualized with DAPI. The insets show microtubule organization at higher magnification.

(C and D) Tomographic reconstruction and 3D modeling of meiotic microtubules in wild-type (C) and *mei-1(null)* (D) mutant. Both tomographic data sets are of equivalent volumes, built from two serial 400 nm sections. The wild-type model shows a portion of one half of the spindle (microtubules in red, pole-proximal ends as white spheres, pole-distal ends as blue spheres, chromatin in green). Pole position (*p*) was determined by examination of serial semithick sections above and below the volume of the half spindle shown here. Both types of ends appear throughout the wild-type spindle, indicating that many individual microtubules within the reconstructed volume terminate before reaching the pole or chromatin surface. Tomographic reconstruction of the *mei-1(null)* mutant revealed a disorganized array of long microtubules.

(E) The number of all microtubules observed within the volume of reconstruction (classes a, b, and c; see inset) for one wild-type and one *mei-1(null)* meiotic sample is shown. The total amount of polymer (μm) within the same volume is also shown.

(F) A histogram displaying the length distribution of microtubules completely contained within the volume of the reconstruction (class c; see inset) is shown. Data were pooled from two different wild-type (white bars) and *mei-1(null)* (gray bars) samples. Scale bars represent 10 μm (B) and 500 nm (D).

katanin resulted in an average of one severing event per 3.01 μm.

We looked in more detail at the morphology of the katanin-induced defects. Of the 316 microtubules shown in Figures 1C and 1E, 138 had lateral defects (holes), most of which also exhibited protofilament curling (Figures 2B and 2C, Movie S4). We also observed closely opposed blunt-ended microtubules having no

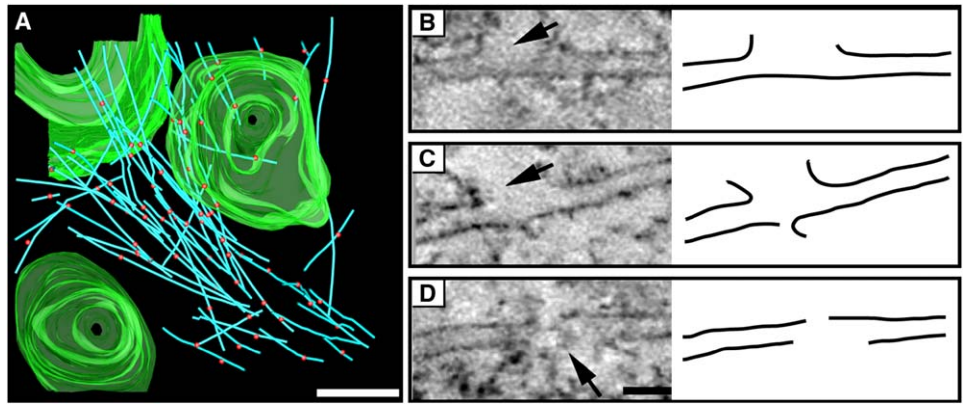

Figure 2. MEI-1 Induces Lateral Defects in Spindle Microtubules

(A) Deconstruction of the 3D model given in Figure 1C to selectively show structural defects in wild-type spindle microtubules. The sites of fragmentation on individual microtubules (blue) are indicated by spheres (red). Numerous microtubules had multiple points of fragmentation along their length.

(B–D) Evidence of microtubule fragmentation. Tomographic slices show (B and C) lateral disruption of the microtubule lattice, and (D) closely opposed microtubule ends. Points of fragmentation are indicated by arrows. Scale bars represent 500 nm (A) and 50 nm (D).

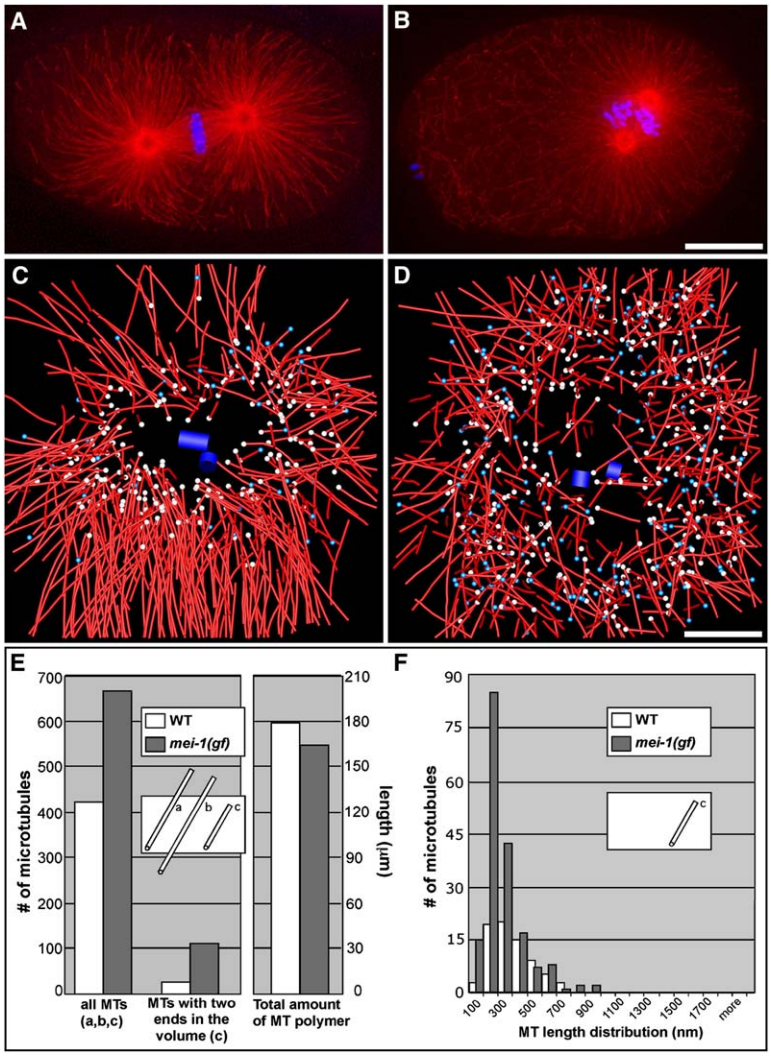

Figure 3. Ectopic MEI-1 Activity Leads to Microtubule Fragmentation in Mitotic Centrosomes

(A and B) Images of mitotic wild-type (A) and *mei-1(gf)* (B) embryos fixed and immunostained with anti-α-tubulin (red) are shown. DNA (blue) is visualized with DAPI. The *mei-1(gf)* spindle is shorter and mispositioned, relative to wild-type.

(C and D) Tomographic reconstruction and 3D modeling of mitotic spindle poles. Wild-type mitotic centrosome (C) and mitotic *mei-1(gf)* centrosome (D) are shown (microtubules, red; pole-proximal ends, white spheres; pole-distal ends, blue spheres; centrioles, blue cylinders).

(E) The number of all microtubules observed within the volume of reconstruction (classes a, b, and c; see inset) for one WT and one *mei-1(gf)* mitotic sample is shown. The total amount of polymer (μm) within the same volume is also shown.

(F) A histogram showing the lengths of microtubules completely contained within the reconstructed volume (class c; see inset) is shown. Data were pooled from two different WT (white bars) and *mei-1(gf)* (gray bars) samples. Scale bars represent 10 μm (B) and 500 nm (D).

obvious protofilament protrusions, although these were relatively rare (i.e., 12/316; Figure 2D). It is possible that the closely opposed microtubule ends represent two unrelated microtubules; however, many were in identical orientations, despite being relatively isolated from neighboring microtubules that might contribute to their alignment. Therefore, we propose that the lateral defects represent the initiation of katanin-mediated severing, and the closely opposed ends represent completely severed microtubules. Breaks in the microtubule lattice could be stress related because the meiotic spindle in *C. elegans* is barrel shaped [10] and the curvature of its microtubules is suggestive of internal tension. However, most of the microtubules having these defects did not exhibit kinking or excessive bending; rather, the microtubules were relatively straight regardless of the extent of damage to their lattice. These data provide structural evidence for meiotic katanin activity in vivo and suggest a molecular mechanism that involves an initial lateral attack on the microtubule lattice, consistent with ATP-dependent formation of katanin oligomers on the lattice [11].

In order to confirm the effect of katanin on microtubule length and polymer number, we used the gain-of-function mutant *mei-1(gf)* to turn on katanin during mitosis [12]. Normally, *C. elegans* katanin is degraded at the end of female meiosis; however, the *mei-1(gf)* mutation prevents this postmeiotic degradation, allowing katanin activity to persist into mitosis [12–14]. In the one-cell embryo, ectopic katanin results in a short, mispositioned mitotic spindle, chromosome segregation defects, and aberrant cytokinesis [12]. In comparison to the wild-type mitotic pole (Figures 3A and 3C; Movie S5), tomographic reconstruction of the *mei-1(gf)* mitotic spindle pole revealed more microtubules surrounding the centrioles (421 versus 667, respectively; Figures 3B, 3D, and 3E; Movie S6). Most of these microtubules were short and randomly oriented and had both their pole-proximal and pole-distal ends contained within the reconstruction, accounting for >3-fold increase in the number of pole-distal ends detected near the *mei-1(gf)* centrosome (111 in *mei-1(gf)* versus 26 in wild-type; Figure 3E). In contrast to the meiotic data, ectopic mitotic katanin did not result in a significant change in the total amount of polymer (Figure 3E). Furthermore, quantification of tubulin by immunofluorescence indicated that *mei-1(gf)* embryos exhibited slightly lower levels of tubulin near the centrosome than wild-type mitotic

embryos (p = 9.7E-04; Figure S1). These data suggest that severed microtubules may be less stable in the mitotic environment. Additional support for this idea is that fewer lateral defects were observed in the mitotic *mei-1(gf)* embryo (22/667), despite a large increase in microtubule fragmentation. One possibility is that the mitotic microtubules are rapidly depolymerized after the severing reaction, making it more difficult to observe early intermediates in the severing process.

To quantify the microtubule length distribution, microtubules having both ends contained within the volume of the reconstruction were measured (179/1294 for *mei-1(gf)* and 74/782 for wild-type; n = 2 poles for each, Figure 3F). The majority of this subset of microtubules in the *mei-1(gf)* mutant were between 200 and 300 nm in length (Figure 3F). Wild-type mitotic poles contained fewer microtubules within the reconstructed volume, and their lengths were slightly more broadly distributed (Figure 3F); this group most likely comprises the subset of actively growing or shrinking microtubules near the wild-type centrosome. In conclusion, ectopic katanin is sufficient to create short microtubules and lattice breaks within mitotic microtubles, although the incidence of lateral defects was lower than what was observed in wild-type meiotic spindles, where katanin is normally active.

Acentrosomal meiotic spindle assembly relies on chromatin-based microtubule nucleation. In *C. elegans* embryos with experimentally compromised centrosome function, chromatin seems to be a relatively inefficient substitute for microtubule nucleation [15–17]. Our data suggest that a major consequence of meiosis-specific katanin activity in *C. elegans* is the conversion of long microtubules into multiple smaller microtubules, thereby increasing the total number of polymers available and allowing for their arrangement during meiotic spindle assembly (Figure 4). Stabilization of severed microtubules might allow polymers to accumulate during meiosis; consistent with this, we observed a net increase in the amount of tubulin polymer in wild-type, compared to *mei-1(null)*. An alternative method to shorten microtubules is to alter microtubule end dynamics, for instance, to increase depolymerization and/or decrease growth rate [18, 19]. This end-wise mechanism, however, would not be expected to significantly change the number of polymers in the system. Katanin-mediated microtubule severing, therefore, provides a means of coordinating the length of microtubules with the density of microtubules in the spindle. Similar mechanisms have also been proposed for the generation of microtubule arrays within acentrosomal plant cells [20] and during the formation of axonal bundles [21].

In vitro experiments and computer modeling have suggested that katanin targets relatively rare defects in the lattice that might arise from changes in protofilament number [22, 23]. Although we cannot directly observe such protofilament variability, this raises the possibility that katanin-severing activity might not necessarily correlate with its distribution pattern or concentration. Consistent with this, we did not observe any bias in the spatial distribution of lattice defects, even though katanin is reportedly most concentrated at the chromatin and poles of the meiotic spindle [9, 12].

Microtubule severing as a mechanism to increase polymer number demands that the newly severed microtubules do not completely depolymerize. It is interesting that katanin activity resulted in an increase in microtubule number in both meiosis and mitosis, but only increased the total polymer amount in meiosis. Our data also suggest that katanin-severed microtubules, on average, are slightly longer in wild-type meiotic spindles than they are in the gain-of-function katanin mitotic centrosomes. Previous work that used UV ablation of

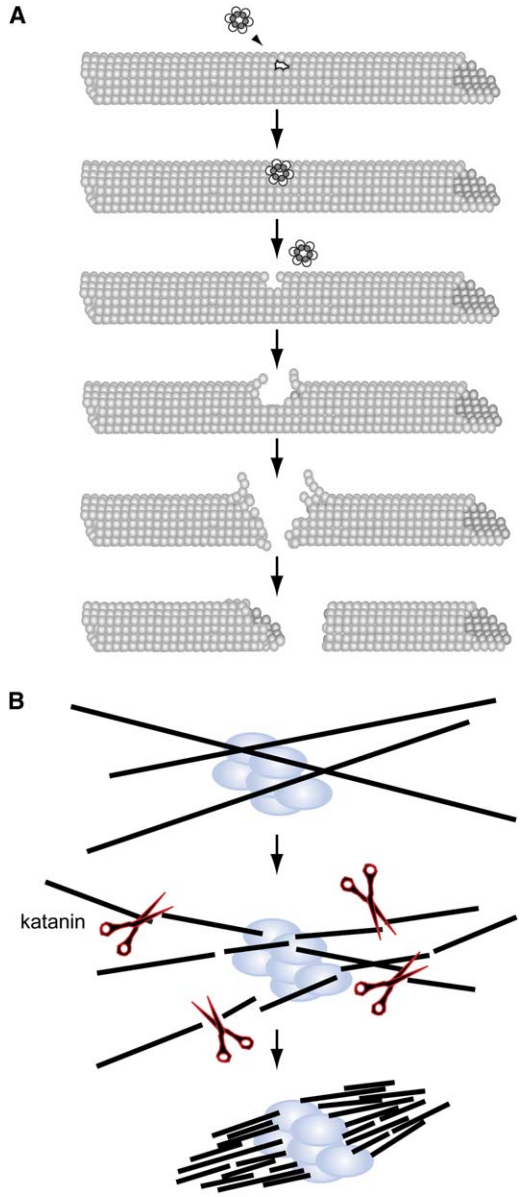

Figure 4. Proposed Model of Katanin's Action and Its Role in Meiotic Spindle Assembly

(A) Katanin (shown as a hexameric ring) may recognize a specific target, such as the pre-existing defect depicted on the microtubule wall. Katanin may also assemble on the microtubule wall (as suggested in [11]). Lateral fragmentation leads to protofilament disruption, subsequent curling, and eventual complete severing of spindle microtubules. Meiotic spindles may contain an activity that inhibits complete depolymerization of the severed microtubules.

(B) During meiotic spindle assembly, severing of microtubules results in an increase in the total number of polymers, which likely facilitates their organization into a bipolar array.

spindles has shown that while minus ends of severed microtubules are quite stable, plus ends rapidly depolymerize back to the poles [24–26]. Although the morphological difference between the meiotic and mitotic pole limits our interpretation, it is possible that severed microtubules are preferentially stabilized during meiosis, or that severed microtubules near the centrosome are more rapidly depolymerized. In this context, the level of katanin activity in frog extracts is inhibited by MAP4 [27]; therefore, cell-cycle-regulated MAPs might also balance the activity of *C. elegans* katanin during meiosis. In addition, at least one candidate that could be involved in promoting the depolymerization of microtubules during mitosis is the depolymerizing kinesin KLP-7, which has been previously implicated in restricting the number of microtubules that grow out from the centrosome [17].

Experimental Procedures

Strains and Culture Conditions

The *mei-1* gene encodes the catalytic subunit of katanin in *C. elegans* [8, 9]. To analyze the *mei-1(null)* mutant embryos, Unc segregants from HR311 *mei-1(ct46ct101) unc-29(e1072)/hT2[bli-4(e937) let(h661)] (I); +/hT2 (III)* were used. *mei-1* gain-of-function mutant embryos were obtained by up-shifting BW729 [*mei-1(ct46ts) unc-29(e1072)* (I)] L4 worms to 25°C. *mei-1(ct46ts)* adult worms were maintained at the restrictive temperature until the high-pressure freezing procedure. For additional details on the genetic properties of these mutant alleles, see [8, 12, 28].

Specimen Preparation

For wild-type and *mei-1(null)* experiments, whole worms were cryoimmobilized with a HPM 010 high-pressure freezer (BAL-TEC) as previously published [29, 30]. For the analysis of wild-type or *mei-1(gf)* mitotic poles, hermaphrodites were cut open in M9 buffer containing 20% BSA. Isolated embryos were collected into capillary tubing, and early developmental events were observed with DIC microscopy. At appropriate stages, capillary tubes containing single embryos were transferred to specimen carriers and rapidly frozen with an EMPACT2+RTS (Leica) [31]. Both whole worms and isolated embryos were freeze-substituted over 2 days at −90°C in anhydrous acetone containing 1% OsO_4 and 0.1% uranyl acetate (EM AFS, Leica). Specimens were subsequently infiltrated and thin-layer embedded in Epon/Araldite. Serial semithick sections (300–400 nm) were cut with a Leica Ultracut UCT Microtome. Sections were collected on Formvar-coated copper slot grids and poststained with 2% uranyl acetate in 70% methanol followed by Reynold's lead citrate.

Intermediate Voltage Electron Tomography

Electron tomography was carried out essentially as described [29, 30]. In brief, 15 nm colloidal gold particles (Sigma-Aldrich) were attached to both surfaces of the semithick sections to serve as fiducial markers for subsequent image alignment. The specimens were placed in a tilt-rotate specimen holder (Gatan, Pleasanton, CA), and tomographic data sets were recorded with a TECNAI F30 intermediate voltage electron microscope (FEI, The Netherlands) operated at 300 kV. Images were captured every 1° over a ±60° range with a Gatan 2K × 2K CCD camera at a pixel size of 1 nm. For the collection of double tilt data sets, the grids were then rotated 90° and a similar tilt series was acquired. For image processing, images were transferred to a Dell Linux workstation and tomograms computed with the IMOD package. In brief, the tilted views were aligned with the positions of the colloidal gold particles as fiducial points. Tomograms were computed for each tilt axis with the R-weighted back-projection algorithm [32]. For double tilt data sets, the two tomograms were aligned to each other and combined [33]. We recorded at least two double-tilt series each for meiotic (wild-type and *mei-1(null)*) and mitotic (wild-type and *mei-1(gf)*) spindle poles. Tomograms were displayed and analyzed with the IMOD software package [34]. This program allows the operator to step through serial slices extracted from the tomogram and to track or model objects of interest in 3D. The ratio of the section thickness, as defined by the microtome's setting to the section's thickness measured after microscopy, was used to calculate a "thinning factor," which was then applied to correct the tomogram's dimension along the beam axis. The lengths of microtubules were then extracted from the model contour data with a companion program, IMODINFO.

Modeling and Analysis of Tomographic Data

With the IMOD software package [34], features like chromosomes, spindle microtubules, and centrioles were modeled in the serial, tomographic slices. An "image slicer" window in IMOD was used to display a slice extracted from the 3D volume in any position or orientation, a tool useful for unambiguous 3D tracking of microtubules [29, 30]. Structural defects of spindle microtubules were analyzed by extracting a slice of image data 1 voxel thick and adjusting its orientation to contain the axis of the microtubule in a single view. A projection of the 3D model was displayed and rotated to study its 3D geometry. For this display in 3D, microtubules were shown as tubular graphic objects. For the quantification of microtubule length in meiotic and mitotic spindle poles, IMODINFO was used to extract the length of microtubules within the volume of the reconstructions. Two meiotic wild-type and two *mei-1(null)* spindles were analyzed. Two poles from independent embryos were analyzed for the wild-type mitotic pole and two poles from the same mutant embryo were used for the *mei-1(gf)* data.

Supplemental Data

Supplemental Data include one figure, six movies, and Supplemental Experimental Procedures and can be found with this article online at http://www.current-biology.com/cgi/content/full/16/19/1944/DC1/.

Acknowledgments

The authors thank P. Mains, C. Cowan, and G. Wiebe for critical reading of the manuscript, P. Mains for worm strains, and J. Mäntler for excellent technical assistance. This work was supported in part by grant RR00592 from the National Center for Research Resources of the National Institutes of Health to J.R. McIntosh, who is a Research Professor of the American Cancer Society.

Received: May 25, 2006
Revised: August 4, 2006
Accepted: August 4, 2006
Published: October 9, 2006

References

1. McNally, F.J., and Vale, R.D. (1993). Identification of katanin, an ATPase that severs and disassembles stable microtubules. Cell *75*, 419–429.
2. Hartman, J.J., Mahr, J., McNally, K., Okawa, K., Iwamatsu, A., Thomas, S., Cheesman, S., Heuser, J., Vale, R.D., and McNally, F.J. (1998). Katanin, a microtubule-severing protein, is a novel AAA ATPase that targets to the centrosome using a WD40-containing subunit. Cell *93*, 277–287.
3. McNally, F.J., and Thomas, S. (1998). Katanin is responsible for the M-phase microtubule-severing activity in *Xenopus* eggs. Mol. Biol. Cell *9*, 1847–1861.
4. Vale, R.D. (1991). Severing of stable microtubules by a mitotically activated protein in *Xenopus* egg extracts. Cell *64*, 827–839.
5. Burk, D.H., Liu, B., Zhong, R., Morrison, W.H., and Ye, Z.H. (2001). A katanin-like protein regulates normal cell wall biosynthesis and cell elongation. Plant Cell *13*, 807–827.
6. Bichet, A., Desnos, T., Turner, S., Grandjean, O., and Hofte, H. (2001). BOTERO1 is required for normal orientation of cortical microtubules and anisotropic cell expansion in *Arabidopsis*. Plant J. *25*, 137–148.
7. Ahmad, F.J., Yu, W., McNally, F.J., and Baas, P.W. (1999). An essential role for katanin in severing microtubules in the neuron. J. Cell Biol. *145*, 305–315.

8. Clark-Maguire, S., and Mains, P.E. (1994). *mei-1*, a gene required for meiotic spindle formation in *Caenorhabditis elegans*, is a member of a family of ATPases. Genetics *136*, 533–546.
9. Srayko, M., Buster, D.W., Bazirgan, O.A., McNally, F.J., and Mains, P.E. (2000). MEI-1/MEI-2 katanin-like microtubule severing activity is required for *Caenorhabditis elegans* meiosis. Genes Dev. *14*, 1072–1084.
10. Albertson, D.G., and Thomson, J.N. (1993). Segregation of holocentric chromosomes at meiosis in the nematode, *Caenorhabditis elegans*. Chromosome Res. *1*, 15–26.
11. Hartman, J.J., and Vale, R.D. (1999). Microtubule disassembly by ATP-dependent oligomerization of the AAA enzyme katanin. Science *286*, 782–785.
12. Clark-Maguire, S., and Mains, P.E. (1994). Localization of the *mei-1* gene product of *Caenorhaditis elegans*, a meiotic-specific spindle component. J. Cell Biol. *126*, 199–209.
13. Pintard, L., Willis, J.H., Willems, A., Johnson, J.L., Srayko, M., Kurz, T., Glaser, S., Mains, P.E., Tyers, M., Bowerman, B., et al. (2003). The BTB protein MEL-26 is a substrate-specific adaptor of the CUL-3 ubiquitin-ligase. Nature *425*, 311–316.
14. Pintard, L., Kurz, T., Glaser, S., Willis, J.H., Peter, M., and Bowerman, B. (2003). Neddylation and deneddylation of CUL-3 is required to target MEI-1/Katanin for degradation at the meiosis-to-mitosis transition in *C. elegans*. Curr. Biol. *13*, 911–921.
15. Dammermann, A., Müller-Reichert, T., Pelletier, L., Habermann, B., Desai, A., and Oegema, K. (2004). Centriole assembly requires both centriolar and pericentriolar material proteins. Dev. Cell *7*, 815–829.
16. Hamill, D.R., Severson, A.F., Carter, J.C., and Bowerman, B. (2002). Centrosome maturation and mitotic spindle assembly in *C. elegans* require SPD-5, a protein with multiple coiled-coil domains. Dev. Cell *3*, 673–684.
17. Srayko, M., Kaya, A., Stamford, J., and Hyman, A.A. (2005). Identification and characterization of factors required for microtubule growth and nucleation in the early *C. elegans* embryo. Dev. Cell *9*, 223–236.
18. Andersen, S.S. (2000). Spindle assembly and the art of regulating microtubule dynamics by MAPs and Stathmin/Op18. Trends Cell Biol. *10*, 261–267.
19. Mitchison, T., and Kirschner, M. (1984). Dynamic instability of microtubule growth. Nature *312*, 237–242.
20. Wasteneys, G.O. (2002). Microtubule organization in the green kingdom: chaos or self-order? J. Cell Sci. *115*, 1345–1354.
21. Baas, P.W., Karabay, A., and Qiang, L. (2005). Microtubules cut and run. Trends Cell Biol. *15*, 518–524.
22. Davis, L.J., Odde, D.J., Block, S.M., and Gross, S.P. (2002). The importance of lattice defects in katanin-mediated microtubule severing in vitro. Biophys. J. *82*, 2916–2927.
23. Chretien, D., Metoz, F., Verde, F., Karsenti, E., and Wade, R.H. (1992). Lattice defects in microtubules: protofilament numbers vary within individual microtubules. J. Cell Biol. *117*, 1031–1040.
24. Leslie, R.J., and Pickett-Heaps, J.D. (1983). Ultraviolet microbeam irradiations of mitotic diatoms: investigation of spindle elongation. J. Cell Biol. *96*, 548–561.
25. Spurck, T.P., Stonington, O.G., Snyder, J.A., Pickett-Heaps, J.D., Bajer, A., and Mole-Bajer, J. (1990). UV microbeam irradiations of the mitotic spindle. II. Spindle fiber dynamics and force production. J. Cell Biol. *111*, 1505–1518.
26. Walker, R.A., Inoue, S., and Salmon, E.D. (1989). Asymmetric behavior of severed microtubule ends after ultraviolet-microbeam irradiation of individual microtubules in vitro. J. Cell Biol. *108*, 931–937.
27. McNally, K.P., Buster, D., and McNally, F.J. (2002). Katanin-mediated microtubule severing can be regulated by multiple mechanisms. Cell Motil. Cytoskeleton *53*, 337–349.
28. Clandinin, T.R., and Mains, P.E. (1993). Genetic studies of *mei-1* gene activity during the transition from meiosis to mitosis in *Caenorhabditis elegans*. Genetics *134*, 199–210.
29. Müller-Reichert, T., Hohenberg, H., O'Toole, E.T., and McDonald, K. (2003). Cryoimmobilization and three-dimensional visualization of *C. elegans* ultrastructure. J. Microsc. *212*, 71–80.
30. O'Toole, E.T., McDonald, K.L., Mantler, J., McIntosh, J.R., Hyman, A.A., and Müller-Reichert, T. (2003). Morphologically distinct microtubule ends in the mitotic centrosome of *Caenorhabditis elegans*. J. Cell Biol. *163*, 451–456.
31. Manninen, A., Verkade, P., Le Lay, S., Torkko, J., Kasper, M., Fullekrug, J., and Simons, K. (2005). Caveolin-1 is not essential for biosynthetic apical membrane transport. Mol. Cell. Biol. *25*, 10087–10096.
32. Gilbert, P.F.C. (1972). The reconstruction of a 3-dimensional structure from projections and its application to electron microscopy. II. Direct Methods. Proc. R. Soc. Lond. B. Biol. Sci. *182*, 89–102.
33. Mastronarde, D.N. (1997). Dual-axis tomography: an approach with alignment methods that preserve resolution. J. Struct. Biol. *120*, 343–352.
34. Kremer, J.R., Mastronarde, D.N., and McIntosh, J.R. (1996). Computer visualization of three-dimensional image data using IMOD. J. Struct. Biol. *160*, 71–76.